Human-like Decision Making and Motion Control for Smooth and Natural Car Following

Chongfeng Wei, *Member, IEEE*, Evangelos Paschalidis, Natasha Merat, Albert Solernou, Foroogh Hajiseyedjavadi, Richard Romano

Abstract— **Car-following is an important driving behaviour for intelligent vehicles and has a significant impact on traffic efficiency and traffic safety. Car-following models are widely developed to characterize the human-drivers' car-following manoeuvre actions and adopted in traffic simulation and automated vehicle control system development. Car-following models need to be able to represent the drivers' behaviour while following preceding vehicles. On the other hand, car-following controllers are an important component of intelligent vehicle systems, both for autonomous vehicles and connected vehicles. However, Adaptive Cruise Control (ACC) as well as Cooperative Adaptive Cruise Control (CACC) do not include human behaviour, which makes their car-following behaviour not human-like or natural for the on-board driver or passenger.**

To address this problem, in this study, the human-like Wiedemann car-following model is calibrated and verified with our driving simulator data. A human-like car-following nonlinear model predictive control (MPC) controller is developed based on the calibrated car-following model. Three different scenarios are tested to evaluate the performance of the proposed controller, with which the autonomous vehicle is able to have human-like and smooth trajectories at different phases and within different transition zones.

Index Terms—**Car-following, Model Predictive Control, Human-like, Calibration, Wiedemann**

I. INTRODUCTION

ONE of the most important objectives in the development of intelligent vehicles is to mitigate traffic congestion. Car-following models are widely developed to characterize the maneuvering actions of human-driven vehicles as well as automated vehicles (AVs) when following a preceding vehicle. These models are quite important for traffic simulation, particularly for a mixed traffic environment consisting of human-driven vehicles and intelligent vehicles. In addition, car-following controllers, developed by researchers to enable automated vehicles are regularly evaluated in car-following scenarios [1-4].

As one of the important aspects of micro traffic simulation, car-following models are developed to replicate the driver's behaviour. With the advent of advanced cruise control, these models have been used to provide the foundation for car-

following control systems. From an engineering perspective, car-following models mostly focus on the driver's physical signals, i.e. time to collision (TTC), velocity, acceleration, distance and their differences between the controlled vehicle and the preceding vehicle [5]. The car-following models can be generally categorized as Linear and car-following (GHR) and improved model [6, 7], Desired measures model [8, 9], Collision avoidance model [10], Optimal velocity model [11, 12], Cellular automata model [13], and Time-space trajectory model [14]. Typically, by assuming each vehicle has an optimal velocity, the acceleration of the following vehicle can be calculated according to the velocity difference between the lead and the following vehicles in the longitudinal direction [15]. However, these models rarely consider the drivers' perception capabilities, psychological reactions, or satisficing tendencies.

To address these problems, some researchers start to involve these human factors into car-following models in order to better explain the human driving behaviour during car-following. Human's reaction time, perception threshold, context sensitivity, desired vehicle states and also driving needs are very important in representing human driven vehicles' driving behaviour [16-18]. Also, more human-like car-following in automated vehicles will make the on-board passenger feel more natural and comfortable. Currently, the most typical car-following model to include these factors is the Wiedemann's model [19], in which the driver's car-following process is divided into several zones: free driving, approaching, and following with unconscious reaction. Particularly, in short spacing scenarios, it defines the deceleration zone and collision zone. This model is widely used in microscopic traffic simulations because it is able to accurately describe the driver's behaviour as different processes [20].

Calibration of existing car-following models is also challenging due to need to collection data for different situations. To evaluate existing car-following models' accuracy, Pourabdollah et al. [21] calibrated and evaluated three different car-following models with data from around 200 recorded trips. Meng et al. [22] measured some key parameters of six typical driver groups and characterised drivers experience and attitude when interacting with risks. To improve the calibration accuracy for car-following models, Rahman et al. [23] applied a stochastic calibration method with regularization

C. Wei, E. Paschalidis, N. Merat, and R. Romano are with the Institute For Transport Studies, University of Leeds, Leeds, LS6 1FH, UK (e-mail: weichongfeng@gmail.com; (E.Paschalidis, N.Merat, A. Solernou, F. Hajiseyedjavadi, R.Romano)@leeds.ac.uk;).
(Corresponding author: Chongfeng Wei, weichongfeng@gmail.com)

to estimate the distribution of parameters of these models. Zhu [24] used naturalistic driving data collected from urban expressways to calibrate the car-following models. However, real world experiments have some limitations as they are not easy to design to meet the researchers' requirements. As an alternative method, a driving simulator provides potential benefits in experiment design and data collection.

Car-following control, normally related to or based on the car-following models, is applied to the longitudinal motion of the vehicle so that some predefined objectives can be achieved. Car-following models are normally used for state feedback or inputs for the control system. To enhance the driving comfort and avoid collisions while following the preceding vehicle, the typical car-following control systems such as Adaptive Cruise Control (ACC) were developed by researchers [2]. However, an ACC algorithm has its own limitations at some severe conditions. When the preceding vehicle moves in an unusual way such as sudden acceleration or deceleration, the preceding vehicle's speed or spacing distance cannot be predicted efficiently. Also, if the preceding vehicle changes its lane or some other vehicles enter into the same lane with the ego vehicle, it will be difficult for the ACC to handle it smoothly. To address these problems, Cooperative Car-following Control (CACC) systems has been developed by involving the information received from the surrounding vehicles [3]. Some other researchers also considered the following cars effect and the merging behaviour of the adjacent vehicle on the host vehicle's car-following performance separately [4, 25-27]. These controllers consider some special conditions during the car-following process, but rarely consider the drivers' perspectives, which make the intelligent vehicle's behaviour not human-like. This may lead to a lack of acceptance by the on-board drivers sitting in the automated vehicles. Human-like control is quite important to improve the on-board users' acceptance of the intelligent vehicles since it can make them feel comfortable and natural [28-30]. Machine learning technology has also been used to develop car-following controllers based on existing test data [31-33]. However, due to the limited test data and the black box characteristics of these models, data-driven AI car-following control development is still at an early stage. Because of these problems, model-based and human-like car-following controller development is quite important.

The importance of human-like autonomous driving techniques have been demonstrated by many researchers, ranging from human-like lane change to human-like motion planning at intersections [28, 29, 34-36]. To reduce the confusion for the other road users and increase the acceptance of the intelligent vehicles from both on-board users and other road users, the behaviour of the intelligent vehicles should to be similarly to human-driven vehicles. To this end, in this study we aim to develop a human-like car-following controller based on a human-centric car-following model calibrated with our driving simulator data.

The contributions of this study are: 1. Calibration of the Wiedemann car following model with human driving car following data collected from the state-of-the-art driving simulator; 2. Development of a human-like car following decision making and control algorithm that can generate comfortable and natural trajectory for the host vehicle, which is the major contribution. The calibrated car following model is used for deriving the car following phases and zones for decision making and constraints for the controller.

II. DATA COLLECTION

A. Experimental design and procedure

The data collection was conducted as part of the HumanDrive project. The University of Leeds Driving Simulator (UoLDS) was used to record driving performance (Fig. 1). The UoLDS has an eight degree of freedom motion base and collects data relating to driver behaviour (vehicle controls), the vehicle (position, speed, accelerations, etc.) and other vehicles in the scene (e.g. identity, position and speed) at a rate of 60Hz. Compared to the real road test environment, simulator-based environment is more flexible and controllable. In this virtual environment, the preceding vehicle's states can be easily defined based on experiment requirement, and the kinematic data of both the host and the preceding vehicles can be collected efficiently and accurately.

Fig. 1. The University of Leeds Driving Simulator (UoLDS)

Driver behaviour was observed in both rural and urban areas, modelled based on real stretches of road in the area of Cranfield around North Bedfordshire. Two loops, North and South were simulated, creating a virtual environment covering around 12 miles of driving. The North loop (top part of Fig. 2) started at the north-western tip of the map in the eastern suburbs of Newport Pagnell. Drivers headed eastwards through the village of North Crawley before turning right towards Wharley End and the Cranfield University campus. The route was 5.6 miles long and took about 15 minutes to complete. The South Loop started close to Martell House (south-eastern tip of the map) and continued westward towards the village of Moulsoe. After passing through Moulsoe, drivers made a 180° U-turn through a roundabout to follow the A509 northbound towards Newport Pagnell. The South Loop also took around 15 minutes to drive.

Each participant undertook six, 15-minute drives, 3xNorth Loop (N) and 3xSouth Loop (S). The order was counterbalanced as either NSNSNS or SNSNSN. During the first pair of drives, participants were accompanied and guided by the researcher for safety reasons. The second pair of drives were undertaken with participants alone in the vehicle. The final pair was also performed alone, but with a leading vehicle (slow moving bus) present for the first half of each Loop in order to observe the participants' car-following behaviour.
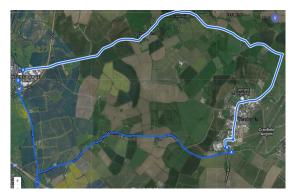
Fig. 2. The full loop of the driving simulator experiment

B. The car-following scenario

The car-following scenario was a part of the last pair of drives. Participants were advised to follow the bus, but they were not allowed to overtake. The task took place for approximately the first half of each loop. In particular, in the North Loop, participants followed the bus from the beginning of the drive until the right turn towards Wharley End (approx. 4.2 miles) and Cranfield University campus. In the South Loop drive, participants followed the bus from the beginning of the Loop until the A509 (approx. 3.1 miles).

C. Sample characteristics

In total, 16 participants were recruited for the purpose of the study, but two of them reported severe motion sickness and withdrew from the study at the stage of the practice drive. From the remaining participants, two more reported motion sickness during the last run (car-following scenario). Of the total sample, eight participants were male and six were female. Minimum age was 28 and maximum 61 years with a mean of 40.29, thus, there were no representatives of a very young age group: 18-24 years old. The average driving experience was approximately 23 years. Finally, six participants reported less than 10,000 miles driven per year, 5 reported exactly 10,000 and only 3 participants exceeded that value.

III. CAR-FOLLOWING MODEL AND PARAMETER DERIVATION

A. The Wiedemann 99 model

The Wiedemann car-following model was originally specified by Rainer Wiedemann [19]. The most recent version of it (Wiedeman 99 model) has been extensively used in the microscopic traffic flow simulation software, VISSIM [37]. The concept of the Wiedemann model is based on the idea of perceptual thresholds. Most of the traditional car-following models assume that drivers are able to notice and react to even the smallest changes of the preceding vehicle behaviour. Wiedemann introduced perceptual thresholds to overcome this drawback. Perceptual thresholds are expressed as a function of relative speed and spacing distance between the following and the preceding vehicle and differ for acceleration and deceleration [5]. The shape of thresholds indicates increased driver alertness when spacing distance is small and provides more freedom when the latter gets larger. The concept of the Wiedemann model is illustrated in Fig. 3.
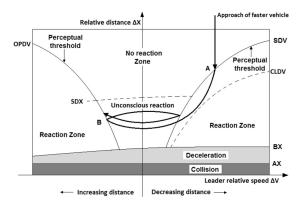

Fig. 3. Perceptual thresholds of the Wiedemann car-following model [5]

The line on the upper right side represents the path of the following vehicle as it is approaching the leader. Initially, the following vehicle is far from the leader and thus it is under a free-flow state. As the vehicle approaches and crosses the deceleration perceptual threshold (SDV), the driver realises that she/he needs to decelerate and match the speed of the preceding vehicle. Given that the driver is not able to actually replicate the behaviour of the preceding vehicle the spacing will increase until the perceptual threshold of acceleration (OPDV). At this point the driver will decelerate again in order to remain at a safe distance. Thus in the car-following state, the following driver keeps oscillating within the perceptual thresholds of acceleration and deceleration, which as shown in Fig. 3 is the unconscious reaction zone.

The Wiedemann 99 model includes 10 main parameters (CC0 to CC9) plus desired speed to approximate car-following behaviour. A description of these parameters are outlined in Section B. Several approaches have been used in literature for the estimation of these parameters. For instance, in a series of studies the Wiedemann model was calibrated using a genetic algorithm (GA) [21, 24, 38]. Other calibration approaches include the direct use of VISSIM [39] optimisation techniques [40] while in [41] a visual based approach was used. In the current paper the latter approach of [41] has been followed to calculate the various parameters of the Wiedemann 99 model. The calculation process is described in more detail in Section B. It should be mentioned that a Genetic Algorithm (GA) framework, similar to the one presented in [24] was tested for the model estimation. However, the visual approach ensures a consistent set of fitting parameters that can be directly fed into the MPC model, while the GA approach results in different sets of parameter values after every model estimation run.

B. The Wiedemann 99 model parameters calculation

Before calculating the Wiedemann model parameters, a car-following region was defined based on the spacing distance-relative speed patterns observed in the data (Fig. 4). Minimum car-following distance was defined as either the 1st or 5th percentile of the spacing distance. The selection of the percentile was based on the car-following pattern of each participant. For participants that always drove above 5.5km/h during the observation period (slow speed very close to standstill condition, [37]) the 1st percentile was considered,

while the 5th percentile was considered for the rest of the cases, in order to avoid deceleration observations before stopping. The upper bound of the car-following distance was either the 90th or the 95th percentile of spacing distance. The decision depended on the initial approaching pattern; the aim was to only keep observations from clear car-following cases and exclude the approaching phase. For the right and left bounds of the car-following areas, the 5th and 95th percentiles of relative speed were considered. The calculation of the various parameters is presented in the next paragraphs.

CC0 is the desired distance the following vehicle aims to keep when both the lead and following vehicles are stationary. This distance was calculated from the South Loop, as the average distance, when and if, both the bus and participant's vehicle were stopped before merging into the A509. A constant value of 3.9236m was calculated and considered identical for all subjects for model validation.

CC1 is the average time headway that the following vehicle desires to keep. The following time headway is translated to a spacing distance calculated as the sum of CC0 and CC1 times following vehicle speed. When following speed gets to its lowest value, the spacing distance represents the minimum safety distance. In the current work, the minimum safety distance was calculated as the 1st or 5th percentile of spacing distance during the car-following task.

The CC2 parameter represents the additional distance over safety distance that a vehicle aims to keep. The CC2 parameter was considered as the distance from the minimum safety distance until the upper bound of the car-following distance.

The CC3 parameter represents the time in seconds from the beginning of the deceleration state until the start of the unconscious car-following state. In the present paper, the value of 4s [41] was considered.
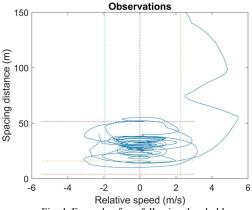

Fig. 4. Example of car-following thresholds

The CC4 and CC5 parameters represent the maximum negative and positive relative speed during the car-following state. Higher values of these parameters indicate that drivers are less sensitive to the preceding vehicle's acceleration/deceleration rates and their speeds vary more during the unconscious following process [41]. The 5th and 95th percentile were considered, in order to avoid outliers or relative speed observations in free-flow or approaching states.

The CC6 parameter represents variation in the following

vehicle's speed oscillation as the spacing headway is increasing. The CC6 parameter has been used to estimate CLDV and OPDV bounds in mathematical functions e.g. [24, 40], however, with reference to [41], changing its value does not significantly affect results. The default VISSIM value of 11.44 was used for the model validation in Section V.

The CC7 parameter captures acceleration during the oscillation (unconscious car-following) process. The CC7 was calculated as the average absolute acceleration values during the car-following process.

The CC8 parameter represents the acceleration when the vehicle starts moving again from stationary position and it was calculated as the 99th percentile of acceleration from a subset of the data below the 5th percentile of speed.

The CC9 parameter represents the acceleration when the vehicle is moving at 80km/h. In the current work, it was calculated as the 99th percentile of acceleration from a subset of data above the 95th percentile of speed.

Finally, the Wiedemann 99 model is also using a parameter to capture the driver's desired speed. In the present paper, the 99th percentile of speed was used for model validation.

IV. CAR-FOLLOWING CONTROLLER DESIGN

A. Vehicle Dynamic Model

As the vehicle is the objective plant that needs to be controlled during car-following manoeuvre, the vehicle model needs to be able to represent its dynamic behaviour as accurately as possible. However, due to the computational cost during the optimization and prediction process of the controller, we choose a 2-dof nonlinear bicycle vehicle model to characterize the vehicle's dynamic behaviour by considering the balance of computation efficiency and model accuracy.

Since we control the vehicle's longitudinal motion based on our calibrated car-following model, the longitudinal space and longitudinal velocity difference between the preceding vehicle and the host vehicle should be predicted. By considering the controller's ability to control the vehicle's lateral movement, we also involve the prediction of the vehicle's states in the lateral direction. Therefore, the state-space model of the vehicle can be expressed by

$$
\begin{cases}
\ddot{y} = -\dot{x}\dot{\psi} + \frac{2}{m}\left(F_{yf}\cos\delta_f - F_{xf}\sin\delta_f + F_{yr}\right) \\
\ddot{x} = \dot{y}\dot{\psi} + a_T \\
\ddot{\psi} = \frac{2}{I_z}\left(l_f(F_{yf}\cos\delta_f + F_{xf}\sin\delta_f) - l_rF_{yr}\right) \\
\dot{e}_y = \dot{y} + \dot{x}e_\psi \\
\dot{e}_\psi = \dot{\psi} - \frac{\dot{x}}{R} \\
\dot{v}_e = a_p - \dot{x} \\
\dot{S}_e = v_e
\end{cases}
\tag{1}
$$

in which $\dot{x}$ and $\dot{y}$ denote the longitudinal and lateral speeds in the body frame, δ_f represent the steer angle of the front wheel, a_T is the longitudinal acceleration input resulting from the external forces, I_z and m represent the vehicle's yaw inertia

and mass, respectively. e_ψ represents the orientation error of the vehicle with respect to the centre line of the lane; e_y represents the lateral position error with respect to the centre line of the lane. l_f and l_r are the vehicle's front and rear axle distances relative the C.G. of the vehicle. R is the curve radius in real time, and $\dot\psi$ denotes the yaw rate. The velocity difference is $v_e = v_{preceding} - v_{host}$, a_p is the acceleration of the preceding vehicle, the spacing distance is $S_e = S_{preceding} - S_{host}$, F_{yf}, F_{xf}, F_{yr} and F_{xr} represent the lateral and longitudinal tyre forces at the front and rear wheels in coordinate frames aligned with the wheels. It is noted that in this study we mainly focus on the vehicle's longitudinal decision making and motion control.

The dynamic equation of the vehicle model can be written in the standard state-space format, which is

$$\dot{\tilde{x}}_s = A_s \tilde{x}_s + B_s u_c \tag{2}$$

where $\tilde{x}_s = [\dot y, \dot x, \psi, \dot\psi, e_y, e_\psi, v_e, S_e]^T$, and the control input $u_c = [\delta_f, a_T]^T$. Since the vehicle dynamic system is a nonlinear system, we need to linearize the system in order that the controller can be designed effectively. If we consider the right side of (2) as $f(\tilde{x}_s, u_c)$, then $A_s = \frac{\partial f(\tilde{x}_s, u_c)}{\partial \tilde{x}_s}\big|_{\tilde{x}_s, u_c}$, $B_s = \frac{\partial f(\tilde{x}_s, u_c)}{\partial u_c}\big|_{\tilde{x}_s, u_c}$.

B. Prediction and Outputs

The proposed vehicle system can be converted into discrete form

$$\tilde{x}_s(k+1) = A_d \tilde{x}_s(k) + B_d u_c(k) \tag{3}$$

The vehicle states $\tilde{x}_s$ at each step can be predicted, and the output can be written as

$$\tilde{y}_d(k) = C_d \tilde{x}_s(k) \tag{4}$$

$$C_d = \begin{bmatrix} 1 & 0 & 0 & 0 & 0 & 0 & 0 & 0 \\ 0 & 1 & 0 & 0 & 0 & 0 & 0 & 0 \\ 0 & 0 & 0 & 1 & 0 & 0 & 0 & 0 \\ 0 & 0 & 0 & 0 & 0 & 0 & 1 & 0 \\ 0 & 0 & 0 & 0 & 0 & 0 & 0 & 1 \end{bmatrix} \tag{5}$$

where A_d, B_d are the discrete matrices for the state-space equations. However, optimization of $\tilde{y}_d$ is not enough to enable the vehicle to have a comfortable trajectory while following the preceding vehicle. The increment of $\tilde{y}_d$ is also important when optimizing the vehicle's performance. For example, longitudinal acceleration, yaw acceleration and the acceleration difference between the host vehicle and the preceding vehicle are important and affect the vehicle's comfort and smoothness during decision making at different stages, i.e. free driving, approaching and unconscious car-following. The increment of the vehicle states and the output can be written as

$$\Delta \tilde{x}_s(k+1) = A_d \Delta \tilde{x}_s(k) + B_d \Delta u_c(k) \tag{6}$$

$$\Delta \tilde{y}_d(k+1) = C_d A_d \Delta \tilde{x}_s(k) + C_d B_d \Delta u_c(k) \tag{7}$$

If we define an augmented vehicle state vector that includes the vehicle states, increment of vehicle states and control inputs that is written as

$$\tilde{x}_e(k) = [\tilde{x}_s(k), \Delta \tilde{x}_s(k), u_c(k-1)]^T \tag{8}$$

Then, the new discrete state-space and extended output equation can be written as

$$\tilde{x}_e(k+1) = A_e \tilde{x}_e(k) + B_e \Delta u_c(k) \tag{9}$$

$$\tilde{y}_e(k) = C_e \tilde{x}_e \tag{10}$$

in which the new coefficient matrix A_e, B_e and C_e can be expressed by

$$A_e = \begin{bmatrix} A_d & O_{8\times8} & B_d \\ O_{8\times8} & A_d & O_{8\times3} \\ O_{3\times8} & O_{3\times8} & I_{3\times3} \end{bmatrix} \tag{11}$$

$$B_e = \begin{bmatrix} B_d \\ B_d \\ I_{3\times3} \end{bmatrix} \tag{12}$$

$$C_e = \begin{bmatrix} C_d & O_{5\times8} & O_{5\times3} \\ O_{3\times8} & C_k & O_{3\times3} \end{bmatrix} \tag{13}$$

in which $O_{p\times q}$ represents a zero matrix with p rows and q columns, I denotes the element matrix, and the matrix C_k is expressed by

$$C_k = \begin{bmatrix} 0 & 1 & 0 & 0 & 0 & 0 & 0 & 0 \\ 0 & 0 & 0 & 1 & 0 & 0 & 0 & 0 \\ 0 & 0 & 0 & 0 & 0 & 0 & 1 & 0 \end{bmatrix} \tag{14}$$

To predict the status of the host vehicle over a fixed prediction horizon N_p, the control increment sequence Δu_c obtained from the MPC is applied to the vehicle model over a control horizon N_c. The future states of the vehicle at $k + N_p$ can be predicted and expressed as [42]

$$\tilde{x}_e(k + N_p) = \prod_{i=0}^{N_p-1} A_e^{(k+i)} \tilde{x}_e(k) +$$

$$\prod_{i=0}^{N_p-2} A_e^{(k+i)} B_e \Delta u_c(k) + \cdots +$$

$$\prod_{i=0}^{N_p-N_c-1} A_e^{(k+i)} B_e \Delta u_c(k + N_c - 1) \tag{15}$$

where $A_e^{(k)}$ represents the coefficient matrix at k, while $A_e^{(k+1)}, A_e^{(k+2)}, \ldots, A_e^{(k+i)}$ represent the matrices in the next i steps.

Therefore, the output expression can be written as [42]

$$\begin{bmatrix} \tilde{y}_e(k+1) \\ \tilde{y}_e(k+2) \\ \vdots \\ \tilde{y}_e(k+N_p) \end{bmatrix} = C_e \Gamma \tilde{x}_e(k) + C_e \Omega \begin{bmatrix} \Delta u_c(k) \\ \Delta u_c(k+1) \\ \vdots \\ \Delta u_c(k+N_c-1) \end{bmatrix} \tag{16}$$

where Γ and Ω are the coefficient matrix derived from (15). In this way, the next N_p steps of the output including vehicle states $\tilde{x}_e$ and its increment can be predicted.

To make the car-following behaviour of the host vehicle human-like, i.e. comfortable, natural and acceptable, we have the following objectives for the dynamic optimisation engineering problem:

• The decision-making and derived host vehicle's trajectory should align with the calibrated car-following model

• From one manoeuvring zone to another manoeuvring zone such as from approaching to following, the trajectory should be as smooth as possible

We set an outer layer and an inner layer for the "unconscious following zone". In the inner layer, the vehicle is allowed to move out in order to have a smooth and comfortable trajectory, when the vehicle moves into the outer layer, it will need to pull back by setting the centre of the "unconscious zone" as the desired state. Their relationship between outer layer and inner layer are defined as

$$\begin{cases} Left_{outer} - Left_{inner} = -1m/s \\ Right_{outer} - Left_{outer} = 1m/s \\ Up_{outer} - Up_{inner} = 5m \\ Down_{outer} - Down_{inner} = -5m \end{cases} \quad (17)$$
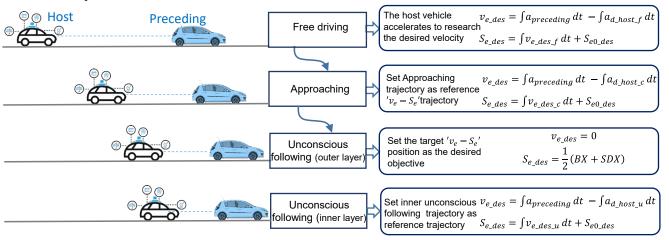

Fig. 5. Decision-making process for the autonomous vehicles with different desired velocity difference (velocity error and spacing)

• During each manoeuvring zone, the vehicle's motion behaviour should be smooth and comfortable

• Within the "unconscious following" phase, the host vehicle does not need to exactly follow the preceding one, i.e. the accelerating behaviour does not need to be synchronous.

To this end, we define different desired velocity differences and spacing to represent the autonomous vehicle's decision-making process in the different phases, as shown in Fig. 5. The vehicle's motion at the 'free driving' zone is not affected by the

In the longitudinal direction, the desired velocity difference and spacing relative to the preceding vehicle can be given by

$$\tilde{x}_{e\_des,long} = [v_{e\_des} , S_{e\_des}]^T \quad (18)$$

where v_{e_des} is the desired velocity error and S_{e_des} is the desired spacing relevant to the preceding vehicle.

In particular, $\tilde{x}_{e\_des,long}$ for difference zones can be written as (19)

$$\tilde{x}_{e\_des,long} =$$
$$\begin{cases} \left[\int a_{preceding}\, dt - \int a_{d\_host\_f}\, dt, \int v_{e\_des\_f}\, dt + S_{e0\_des}\right]^T & if\ -v_e < SDV\ and\ S_e > SDX \quad (\textbf{c1}) \\ \left[\int a_{preceding}\, dt - \int a_{d\_host\_a}\, dt, \int v_{e\_des\_c}\, dt + S_{e0\_des}\right]^T & if\ SDV < -v_e < CLDV\ and\ S_e > BX \quad (\textbf{c2}) \\ \left[0, \frac{1}{2}(BX + SDX)\right]^T & if\ OPDV + 1 < -v_e < SDV - 1\ and\ BX + 5 < S_e < SDX - 5 \quad (\textbf{c3}) \\ \left[\int a_{preceding}\, dt - \int a_{d_{host_u}}\, dt, \int v_{e_{des_u}}\, dt + S_{e0_{des}}\right]^T & OPDV < -v_e < SDV\ and\ BX < S_e < SDX\ exclude\ \textbf{c3} \quad (\textbf{c4}) \end{cases} \quad (19)$$

preceding vehicle. Instead, the host vehicle accelerates to reach the desired velocity, and in this period we assume the on-board drivers have not perceived the speed difference between the host vehicle and the preceding one. When the vehicle moves into the 'approaching' zone, it is expected that the vehicle is able to track the desired $'v_e - S_e'$ trajectory derived by the calibrated car-following model. When the vehicle state enters into the 'unconscious following' zone, the objective of the host vehicle's state is changed to keep its moving smooth unless the preceding vehicle has a high accelerating or braking behaviour.

where S_{e0_des} represents the initial spacing between the host vehicle and the preceding one, $a_{preceding}$ is the acceleration of the preceding vehicle , $v_{e\_des\_f}$ and $v_{e\_des\_c}$ are desired velocity of the host vehicle in the free driving zone and approaching zone respectively. $a_{d\_host\_f}$ is the desired acceleration of the host vehicle in the free driving zone, $a_{d\_host\_a}$ is the desired acceleration of the host vehicle in the approaching zone,

$a_{d\_host\_u}$ is the desired acceleration of the host vehicle in the inner layer of unconscious zone, which can be written as

$$a_{d\_host\_a} = \frac{1}{2} \frac{v_e^2}{\left(AX(t) - (S_e - L_{preceding})\right)} + a_{preceding}(t) \qquad (20)$$

$$a_{d\_host\_f} = \begin{cases} CC7 & if\ v_{ego} > VDES \\ \min(a_{max}, VEDS - v_{ego}) & if\ v_{ego} \le VDES \end{cases} \qquad (21)$$

$$a_{d\_host\_u} = \\ \begin{cases} \min(a_{preceding}, -CC7) & if\ a_{preceding} < 0 \\ \min(\max(a_{preceding}, CC7), VEDS - v_{preceding}) & if\ a_{preceding} \ge 0 \end{cases} \qquad (22)$$

where $\tilde{y}_{des}(k + i)$ is the desired output of the host vehicle, Q and R are weighting matrices of appropriate dimensions, ρ represents the weight coefficient, ε is the relaxation factor. The involvement of the slack variable is to avoid the case that the optimal solution is not obtained within the calculation time. Eq. (27) and (28) are the constraints on the acceleration and its increment, which are designed to control the host vehicle's jerky behaviour and make the trajectory smooth, particularly for the transitions from one zone to another. (29) and (30) represent the constraints that limit the vehicle states into the

Table 2 Descriptive statistics of the car-following parameters

	CC1	CC2	CC4	CC5	CC7	CC8	CC9	VDES	Safety distance
min	1.9653	20.7898	-4.0077	1.4620	0.2289	0.6944	-0.0783	17.5000	8.0984
max	6.7907	93.2946	-1.7259	3.4957	0.3792	3.1821	1.5731	29.6688	43.8152
median	3.0119	41.9846	-2.2623	1.9319	0.3024	1.5154	0.7248	19.3776	20.1035

where $a_{max} = CC8 + 0.02\ CC9 \min(v_{ego}, VDES)$.

When the states of the host vehicle enter into the 'unconscious following' zone, the vehicle will be limited into the zone and not allowed to move out of the zone except in some special conditions, i.e. the constraints of the vehicle states will be automatically set as the boundaries of this zone unless the preceding vehicle accelerates greater than $1\ m/s^2$. The velocity difference and displacement difference between the host and the preceding vehicles are expressed as

$$[v_e, S_e]^T \in [\mathcal{L}, \mathcal{H}]^T \quad if\ SDV < -v_e < CLDV\ \&\ S_e > BX \qquad (23)$$

$$[v_e, S_e]^T \in [\Re, \Im]^T \quad if\ OPDV < -v_e < SDV\ \&\ BX < S_e < SDX \qquad (24)$$

where $\mathcal{L}$ represent all the real number between SDV and $CLDV$, $\mathcal{H}$ represent all the real number higher than BX, $\Re$ represents all the real number between $OPDV$ and SDV, and $\Im$ represents all the real number between BX and SDX.

In addition to constraints on the desired vehicle states in the phases (zones), the host vehicle's longitudinal acceleration and the jerk effect (i.e. acceleration increment) are constrained to enable the vehicle to have a smooth trajectory during transition between two different zones and limit the vehicle's oscillation behaviour. The human-like car following MPC problem can be synthesized as follows:

$$\min_{\Delta u_c(t)} J(\tilde{x}_e(k), \Delta u_c(k)) = \sum_{i=1}^{N_p} \left\| \tilde{y}_e(k + i) - \tilde{y}_{des}(k + i) \right\|_Q^2 + \sum_{i=1}^{N_c-1} \left\| \Delta u_{k+i} \right\|_R^2 + \rho\varepsilon^2 \qquad (25)$$

$$\tilde{x}_e(k + i + 1) = A_e\tilde{x}_e(k + i) + B_e u_c(k + i), \quad i = 0,1,\dots,N_p - 1 \qquad (26)$$

$$u_{c_{min}} \le u_{k+i,t} \le u_{c_{max}}, \quad i = 0,1,\dots,N_c - 1 \qquad (27)$$

$$\Delta u_{c_{min}} \le \Delta u_{k+i,t} \le \Delta u_{c_{max}}, \quad i = 0,1,\dots,N_c - 1 \qquad (28)$$

$$[v_e, S_e]^T \in [\mathcal{L}, \mathcal{H}]^T \quad if\ SDV < -v_e < CLDV\ and\ S_e > BX \qquad (29)$$

$$[v_e, S_e]^T \in [\Re, \Im]^T \quad if\ OPDV < -v_e < SDV\ and\ BX < S_e < SDX \qquad (30)$$

specific zones during approaching and following the preceding vehicle.

V. CAR-FOLLOWING MODEL PARAMETER ESTIMATES

A. Parameter results

Different sets of parameters were calculated for each participant and each Loop. However, because of issues in the data recording, the data for the bus was not recorded for several participants. In total, 7 valid cases were considered from the North loop and 6 from the South loop. The results of the valid cases are presented in Table 1. Moreover, the descriptive statistics of the parameters are outlined in Table 2.

Table 1 Model validation indices

ID	Loop	Wilcoxon rank sum p-values		RMSPE	
		Speed	Spacing distance	Speed	Spacing distance
1	North	0.000	0.000	0.265	0.470
1	South	1.000	0.000	0.302	0.500
2	North	0.000	0.000	0.160	0.448
2	South	0.123	0.000	0.280	0.502
3	North	0.259	0.000	0.198	0.425
3	South	0.024	0.000	0.204	0.353
4	North	0.691	0.000	0.156	0.532
4	South	0.204	0.000	0.162	0.500
8	North	0.079	0.000	0.149	0.544
10	North	0.008	0.000	0.169	0.473
10	South	0.092	0.000	0.196	0.644
12	South	0.285	0.459	0.125	0.447
13	North	0.117	0.000	0.232	0.381

The CC0 value was considered identical for all participants equal to 3.9236m while the median safety car-following distance was calculated as 20.1035m. The time headway parameter (CC1) had a median value of 3.0119s across all participants. This value is higher than previous literature

however, it should be mentioned that the data used in the current work refer to a rural/urban environment rather than motorway data that is usually used in car-following model estimation. The median values of negative (CC4) and positive (CC5) relative speed thresholds were -2.2623 and 1.9319 respectively. Finally, the median car-following acceleration (CC7) was calculated as 0.3024m/s^2.

B. Parameter validation per individual

In order to validate the calculated parameters, the parameters of each individual were separately used in a car-following model based on the principles of the Wiedemann 99 model. This model was tested in a car-following situation with a vehicle following a bus, as participants did in the car-following driving simulator scenarios. The details of the model specification have been described in detail in [24]. For each individual, the observed versus predicted plots of speed and spacing distance cumulative distributions were compared. An example for a single individual is illustrated in Fig. 6. Moreover, the Wilcoxon rank-sum test was used to compare whether the central tendency of these distributions was significantly different while a variant of the root-mean-square percentage-errors (RMSPE) was used as a relative indicator of model fit. The latter is defined as

$$\text{RMSPE} = \sqrt{\frac{\sum_{i=1}^{N}\left(X_i^{sim} - X_i^{obs}\right)^2}{\sum_{i=1}^{N}\left(X_i^{obs}\right)^2}} \qquad (31)$$

where X_i^{obs} is a variable (e.g. speed or spacing distance) as observed in the data while X_i^{sim} is the same variable as predicted by the model. The detailed results are presented in Table 1. Finally, an example of observed versus predicted Spacing distance-Relative speed patterns are illustrated in Fig. 7.

As shown in Table 1, the p-value results of the Wilcoxon rank-sum test were insignificant for most of the cases individuals which shows that the medians of the observed versus the simulated distributions of speed were not significantly different in these cases. However, with respect to spacing distance, the p-values were below 0.05, except for one case, indicating that the median values between observed and predicted spacing distances were significantly different.
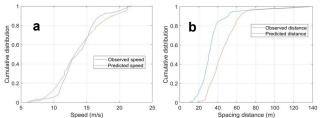

Fig. 6. Observed vs predicted cumulative distributions of: (a) speed and (b) spacing distance
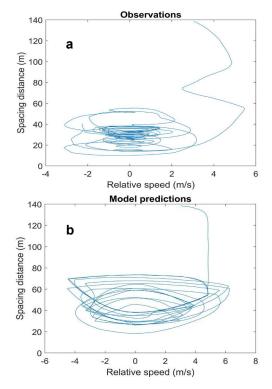

Fig. 7. Relative speed - Spacing distance behaviour: (a) Observed and (b) Predicted curves

VI. CAR-FOLLOWING CONTROL RESULTS AND DISCUSSION

To assess the performance of the car-following controller, we choose three scenarios for simulation and analysis: 1. The preceding vehicle has a constant speed; 2. The preceding vehicle's speed and acceleration data was obtained from the human-driven vehicle data in the UoL driving simulator environment; 3. The preceding vehicle's data is from the bus trajectory that was used for car-following test.

For the first scenario, the preceding vehicle has a speed of 15 m/s while the host one has a speed of 20 m/s, and the spacing distance between them is 180 m. The obtained $'v_e - S_e'$ trajectory of the host vehicle relative to the preceding vehicle is shown in Fig. 8. It can be seen during the 'free driving' zone, the vehicle nearly keeps its original speed until it enters into the 'approaching' zone. Within the 'approaching' zone, the host automated vehicle smoothly reduces the relative velocity difference between the host vehicle and the preceding vehicle. Within the 'unconscious following' zone, the vehicle optimises its relative speed and spacing difference to arrive at the expected final states, i.e. zero relative speed and data-driven human-like spacing distance, and keep the states stable.
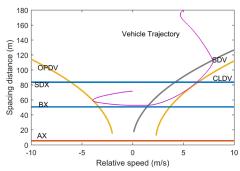
Fig. 8. The host vehicle's $'v_e - S_e'$ trajectory relative to preceding vehicle with a constant speed.

For the second scenario, the preceding vehicle is assumed to have a constant velocity at the beginning and has a frequent variation in velocity after the following vehicle starts to follow it. The aggressive driving style can be characterised by quick or frequent lane changes, braking and acceleration [43]. Therefore, the preceding vehicle's behaviour can be considered as aggressive driving during car-following period.
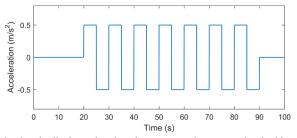

Fig. 9. longitudinal acceleration data representing aggressive braking and accelerating behaviour

With the proposed controller, the planned vehicle trajectory can be seen in Fig. 9. Within the following zone, the host vehicle attempts to tune its speed smoothly and naturally, rather than exactly keeping the same speed as the preceding vehicle, which changes speed frequently. This behaviour is consistent with the human-driven vehicle's car following behaviour, i.e. preferring changing speed smoothly and naturally during car following instead of changing speed simultaneously with the preceding aggressive vehicle.
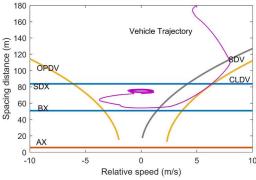

Fig. 10. The host vehicle's $'v_e - S_e'$ trajectory relative to preceding vehicle with an aggressive driving behaviour

For the third scenario, we adopted the human-driven data collected from our UoLDS environment. The vehicle's initial speed (15.1 m/s) and acceleration profile were taken to characterise the preceding vehicle's trajectory. Fig. 9 shows the preceding vehicle's acceleration profile, from which its velocity and distance can be generated. The host vehicle's speed is set as 19 m/s, and initial spacing distance is set as 150 m.
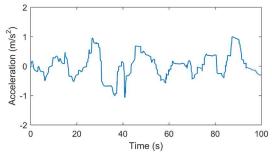

Fig. 11. Human-driven longitudinal acceleration data collected from our UoLDS environment

The derived 'relative speed-spacing distance' trajectory based on the MPC control system is shown in Fig. 10. The host vehicle's trajectory shows that the vehicle is able to arrive at the expected final state through a human-like manoeuvrability phase, i.e. keep free driving, and close in on the preceding vehicle until it is ready to follow the vehicle incautiously. It is also found the smoothness of the trajectory during the transitions between different zones are quite high compared to Fig. 7(b). When the vehicle moves into the "unconscious zone", it starts to move into the innver layer from the outer layer, and tune the relative speed and spacing distance based on receiving a smooth trajectory and low acceleration variation.
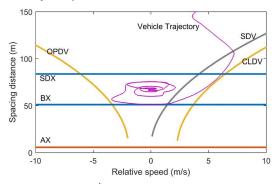

Fig. 12. The host vehicle's $'v_e - S_e'$ trajectory relative to preceding vehicle with human-driven vehicle data winthin the UoLDS environment.
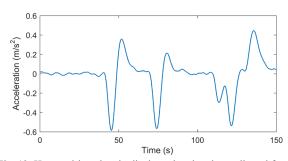

Fig. 13. Human-driven longitudinal acceleration data collected from Aimsun transport simulation
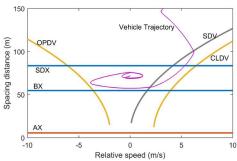
Fig. 14. The host vehicle's $'v_e - S'_e$ trajectory relative to preceding bus's movement

In the fourth scenario, we adopted the bus's trajectory as it always happened in the experiment, and the bus's acceleration and initial velocity data adopted here is from the Aimsun transport data, as shown in Fig. 11. The spacing distance and the initial speed of the host vehicle are set the same as our driving test, which are 149.96 m and 19.57 m/s, and the lead bus's initial velocity is 16.33 m/s. The host vehicle's trajectory derived from the MPC is shown in Fig. 12, in which the relative speed and the spacing distance relative to the lead bus's motion are demonstrated. It can be seen that the vehicle's trajectory is smooth during the whole phase even if the lead bus has a high variation of speed. Particularly, when the vehicle moves into the inner layer of the "unconscious zone", it starts to tune its acceleration and moves smoothly within the inner layer, and it does not move out since the preceding vehicle's acceleration is within a small range typically less than CC7.

Different from the human-driven vehicle's car-following performance described in Fig. 7, the automated vehicle moves smoothly and comfortably at different phases and within different zones. Particularly, the vehicle's performance within the "unconscious following" zone is much smoother than what was derived from original Wiedemman model as shown in Fig. 7. This will enable the on-board drivers' to have a more natural and comfortable driving experience. This demonstrates that the proposed controller is able to make a human-like but smoother driving experience for the on-board drivers during car-following.

To compare the automated vehicle's $'v_e - S'_e$ trajectory with the human-driven vehicle's trajectory, we choose two measured human-driven car following data for two different road routes, which were captured from the area of Cranfield in the UK and regenerated the surrounding environment and the road in the simulator environment (UoLDS), as shown in Fig.15. Both of the two drivers followed a bus at two different road sections.

It can be seen both the two drivers follow the preceding vehicle with three phases: free driving to get to a point that the drivers they can perceive the speed difference between the preceding vehicle and the host vehicle; closing in phase to make the host vehicle moves into an acceptable distance range between the preceding vehicle and the host vehicle; keeping unconscious following within the acceptable distance and speed ranges. All of the planned trajectories, scenario 1 to scenario 4, generated by the proposed decision making and control algorithm have the similar three phases, i.e. free driving to

detect the speed difference, closing in phase and unconscious following phase. The second human-like property is that all the trajectories for the four scenarios show smooth transitions between two different phases, which is similar to the human-driven vehicles. When the vehicle moves into the unconscious following zone, the proposed system holds the automated vehicle inside the acceptable zone while minimising the acceleration, rather than keeping the exact same speed and constant distance compared to the preceding vehicle, in which case the vehicle will stay at a fixed $'v_e - S'_e$ point. Both the planned vehicle trajectory using the proposed algorithm and the measured human-driven vehicle's car following data show this phenomenon. Therefore, the automated vehicle with the proposed decision making and control algorithm shows a human-like behaviour during car following.
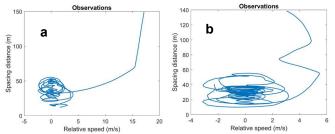

Fig. 15. Measured human-driven car following data for different routes using the UoLDS. (a) Driver #1 in the South loop of the area of Cranfield, (b) Driver #2 in the North loop of the area of Cranfield.
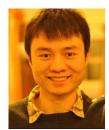
VII. CONCLUSIONS

In this study, we proposed a method to calibrate the Wiedemann car-following model with the driving simulator data. Different road type and conditions were used to derive the parameters of the car-following model. The relative speed and spacing distance predicted by the calibrated model align well with the observed speed and spacing data.

Based on the calibrated car-following model, we developed a decision-making and vehicle motion control algorithm, and a nonlinear MPC controller was designed to determine and optimise the host automated vehicle's behaviour while following the preceding vehicles. Three different scenarios, i.e. constant speed preceding vehicle, human-driven preceding vehicle, and variable-speed lead bus, were tested in the simulation environment to assess the performance of the proposed algorithm and the controller. All the results within the three scenarios have shown satisfactory performance in terms of smoothness, human-like characteristics and stabilities. In particular, the controller is able to realize human-like behaviour during car-following, making different decisions for different phases and within different zones, which can make the on-board drivers feel natural and comfortable. In addition, the automated vehicle has smooth and natural motion behaviour during transitions between the 'free driving', 'approaching' and 'unconscious following' zones.

REFERENCES

[1] A. Ghaffari, B. Gharehpapagh, A. Khodayari, and S. Salehinia, "Longitudinal and lateral movement control of car following maneuver using fuzzy sliding mode control." *IEEE 23rd ISIE*, pp. 150-155, 2016

[2] W. Li, T. Chen, J. Guo, and J. Wang, "Adaptive Car-Following Control of Intelligent Electric Vehicles." *IEEE 4th ICCSSE*, pp. 86-89, 2018

[3] M. Wang, W. Daamen, S. P. Hoogendoorn, and B. v. Arem, "Cooperative Car-Following Control: Distributed Algorithm and Impact on Moving Jam Features," *IEEE Transactions on Intelligent Transportation Systems,* vol. 17, no. 5, pp. 1459-1471, 2016.

[4] M. Wang, S. P. Hoogendoorn, W. Daamen, B. van Arem, and R. Happee, "Game theoretic approach for predictive lane-changing and car-following control," *Transportation Research Part C: Emerging Technologies,* vol. 58, pp. 73-92, 2015.

[5] M. Saifuzzaman, and Z. Zheng, "Incorporating human-factors in car-following models: A review of recent developments and research needs," *Transportation Research Part C: Emerging Technologies,* vol. 48, pp. 379-403, 2014.

[6] R. E. Chandler, R. Herman, and E. W. J. O. r. Montroll, "Traffic dynamics: studies in car following," *Operations Research,* vol. 6, pp. 165-184, 1958.

[7] K. I. Ahmed, "Modeling drivers' acceleration and lane changing behavior," Massachusetts Institute of Technology Thesis, 1999.

[8] M. Treiber, A. Hennecke, and D. Helbing, "Congested traffic states in empirical observations and microscopic simulations," *Physical Review E,* vol. 62, pp. 1805-1824, 2000.

[9] M. Treiber, and D. Helbing, "Memory effects in microscopic traffic models and wide scattering in flow-density data," *Physical Review E,* vol. 68, no. 4, pp. 046119, 2003.

[10] J. Barceló, and J. Casas, "Dynamic Network Simulation with AIMSUN," *Simulation Approaches in Transportation Analysis*, R. Kitamura and M. Kuwahara, eds., pp. 57-98, Boston, MA: Springer US, 2005.

[11] L. C. Davis, "Modifications of the optimal velocity traffic model to include delay due to driver reaction time," *Physica A: Statistical Mechanics and its Applications,* vol. 319, pp. 557-567, 2003.

[12] H. Gong, H. Liu, and B.-H. Wang, "An asymmetric full velocity difference car-following model," *Physica A: Statistical Mechanics and its Applications,* vol. 387, pp. 2595-2602, 2008.

[13] Z. Zheng, "Recent developments and research needs in modeling lane changing," *Transportation Research Part B: Methodological,* vol. 60, pp. 16-32, 2014.

[14] Z. Zheng, S. Ahn, D. Chen, and J. Laval, "The effects of lane-changing on the immediate follower: Anticipation, relaxation, and change in driver characteristics," *Transportation Research Part C: Emerging Technologies,* vol. 26, pp. 367-379, 2013.

[15] M. Bando, K. Hasebe, A. Nakayama, A. Shibata, and Y. Sugiyama, "Dynamical model of traffic congestion and numerical simulation," *Physical Review E,* vol. 51, pp. 1035-1042, 1995.

[16] S. Hamdar, "Driver Behavior Modeling," *Handbook of Intelligent Vehicles*, A. Eskandarian, ed., pp. 537-558, London: Springer London, 2012.

[17] M. Treiber, and A. Kesting, "Car-Following Models Based on Driving Strategies," *Traffic Flow Dynamics: Data, Models and Simulation*, M. Treiber and A. Kesting, eds., pp. 181-204, Berlin, Heidelberg: Springer Berlin Heidelberg, 2013.

[18] S. H. Hamdar, H. S. Mahmassani, and M. Treiber, "From behavioral psychology to acceleration modeling: Calibration, validation, and exploration of drivers' cognitive and safety parameters in a risk-taking environment," *Transportation Research Part B: Methodological,* vol. 78, pp. 32-53, 2015.

[19] R. Wiedemann, "Simulation des Strassenverkehrsflusses," 1974.

[20] M. Mai, L. Wang, and G. Prokop, "Advancement of the car following model of Wiedemann on lower velocity ranges for urban traffic simulation," *Transportation Research Part F: Traffic Psychology and Behaviour,* vol. 61, pp. 30-37, 2019.

[21] M. Pourabdollah, E. Bjärkvik, F. Fürer, B. Lindenberg, and K. Burgdorf, "Calibration and evaluation of car following models using real-world driving data." *IEEE 20th ITSC*, pp. 1-6, 2017.

[22] F. Meng, W. Zhang, and J. Wang, "Driver's car-following and lane-changing models: An experimental study." *IEEE 22nd ICIEEM*, pp. 2045-2048, 2011.

[23] M. Rahman, M. Chowdhury, T. Khan, and P. Bhavsar, "Improving the Efficacy of Car-Following Models With a New Stochastic Parameter Estimation and Calibration Method," *IEEE Transactions on Intelligent Transportation Systems,* vol. 16, pp. 2687-2699, 2015.

[24] M. Zhu, X. Wang, A. Tarko, and S. e. Fang, "Modeling car-following behavior on urban expressways in Shanghai: A naturalistic driving study," *Transportation Research Part C: Emerging Technologies,* vol. 93, pp. 425-445, 2018.

[25] Y. Guo, Q. Sun, R. Fu, and C. Wang, "Improved Car-Following Strategy Based on Merging Behavior Prediction of Adjacent Vehicle From Naturalistic Driving Data," *IEEE Access,* vol. 7, pp. 44258-44268, 2019.

[26] J. Yao, Q. Jia, and L. Shen, "Pinning control of a new car-following model with the consideration of preceding and following cars." *IEEE CCA,* pp. 816-821, 2015.

[27] Y. Zhang, Q. Lin, J. Wang, S. Verwer, and J. M. Dolan, "Lane-Change Intention Estimation for Car-Following Control in Autonomous Driving," *IEEE Transactions on Intelligent Vehicles,* vol. 3, pp. 276-286, 2018.

[28] Y. Gu, Y. Hashimoto, L.-T. Hsu, M. Iryo-Asano, and S. Kamijo, "Human-like motion planning model for driving in signalized intersections," *IATSS Research,* vol. 41, pp. 129-139, 2017.

[29] C. Wei, R. Romano, F. Hajiseyedjavadi, N. Merat, and E. Boer, "Driver-centred Autonomous Vehicle Motion Control within A Blended Corridor," *IFAC-PapersOnLine,* vol. 52, pp. 212-217, 2019.

[30] C. Wei, R. Romano, N. Merat, F. Hajiseyedjavadi, A. Solernou, E. Paschalidis, and E. R. Boer, "Achieving Driving Comfort of AVs by Combined Longitudinal and Lateral Motion Control." 26th *IAVSD,* pp. 1107-1113, 2019.

[31] V. Papathanasopoulou, and C. Antoniou, "Towards data-driven car-following models," *Transportation Research Part C: Emerging Technologies,* vol. 55, pp. 496-509, 2015.

[32] D. Yang, L. Zhu, Y. Liu, D. Wu, and B. Ran, "A Novel Car-Following Control Model Combining Machine Learning and Kinematics Models for Automated Vehicles," *IEEE Transactions on Intelligent Transportation Systems,* vol. 20, pp. 1991-2000, 2019.

[33] M. Zhu, X. Wang, and Y. Wang, "Human-like autonomous car-following model with deep reinforcement learning," *Transportation Research Part C: Emerging Technologies,* vol. 97, pp. 348-368, 2018.

[34] L. Li, K. Ota, and M. Dong, "Humanlike Driving: Empirical Decision-Making System for Autonomous Vehicles," *IEEE Transactions on Vehicular Technology,* vol. 67, pp. 6814-6823, 2018.

[35] D. S. González, M. Garzón, J. S. Dibangoye, and C. Laugier, "Human-Like Decision-Making for Automated Driving in Highways." *IEEE ITSC,* pp. 2087-2094, 2019.

[36] P. Wang, D. Liu, J. Chen, H. Li, and C.-Y. J. a. Chan, "Human-like Decision Making for Autonomous Driving via Adversarial Inverse Reinforcement Learning," arXiv: 1911.08044, 2019.

[37] P. Vissim, "7–USER MANUAL, 2015," *Karlsruhe, Njemačka.* 2015

[38] B. Higgs, M. Abbas, and A. Medina, "Analysis of the Wiedemann car following model over different speeds using naturalistic data." *3rd International Conference on Road Safety and Simulation*, pp. 1-22, 2011.

[39] M. Fellendorf, and P. Vortisch, "Validation of the microscopic traffic flow model VISSIM in different real-world situations." *Transportation Research Board 80th Annual Meetingm,* 2001.

[40] K. Aghabayk, M. Sarvi, W. Young, and L. Kautzsch, "A novel methodology for evolutionary calibration of Vissim by multi-threading." *ATRF 2013 - Proceedings*, pp. 1-15. 2013

[41] U. Durrani, C. Lee, and H. Maoh, "Calibrating the Wiedemann's vehicle-following model using mixed vehicle-pair interactions," *Transportation Research Part C: Emerging Technologies,* vol. 67, pp. 227-242, 2016.

[42] C. Wei, R. Romano, N. Merat, Y. Wang, C. Hu, H. Taghavifar, F. Hajiseyedjavadi, and E. R. Boer, "Risk-based autonomous vehicle motion control with considering human driver's behaviour," *Transportation Research Part C: Emerging Technologies,* vol. 107, pp. 1-14, 2019.

[43] E. M. Szumska, and R. Jurecki, "The Effect of Aggressive Driving on Vehicle Parameters," *Energies*, vol. 13, pp. 6675, 2020.

Chongfeng Wei received his Ph.D. degree in mechanical engineering from the University of Birmingham, Birmingham, U.K., in 2015. He was a research fellow at University of Leeds, and now a senior lecturer at Northumbria University, UK. His current research focuses on Human-centric Autonomous Driving including Human-like Automated Vehicle Control and Human-centric Decision Making, Motion Planning and Control for Intelligent Vehicles.

Evangelos Paschalidis has a Diploma in Rural and Surveying Engineering (2012) and a MSc in Transport planning (2013), both from the Aristotle University of Thessaloniki, Greece. He received his PhD at University of Leeds in 2019. He is currently working as a research fellow in the Innovate UK-funded project HumanDrive at the Institute for Transport Studies, University of Leeds. His research interests are related to traffic psychology, driving behaviour, econometrics and discrete choice modelling.

Natasha Merat has a BSc in Physiology and a PhD in Psychology, both from the University of Leeds and is research group leader and chair professor of the Human Factors and Safety Group, @ITS Leeds. Her main research interests are in understanding the interaction of road users with new technologies. She applies this interest to studying factors such as driver distraction and driver impairment, and she is an internationally recognised expert in studying the human factors implications of highly automated vehicles.

Albert Solernou Crusat hold a degree in physics and a PhD in physical chemistry about the energy landscape of protein-protein interactions developed at the Barcelona Supercomputing Center.

He has became the Advanced Research Computing Officer, and now focus on the computing system and environment development for the driving simulator, and computational simulation for automated driving.

Foroogh Hajiseyedjavadi received the B.Sc. in Civil Engineering from the Sharif University of Technology, in 2012. She received her MSc and PhD in Transportation Engineering at the University of Massachusetts Amherst, working on driver behavior studies. Since 2018, she has been a research fellow at the Institute for Transport Studies at the University of Leeds working on driver behavior analysis.

Richard Romano received the Ph.D. degree in industrial engineering from the University of Iowa, Iowa City, IA, USA, 1999. He is currently the Chair Professor of driving simulation in the Institute for Transport Studies at the University of Leeds, Leeds, U.K. His current research interests include motion cueing algorithms, vehicle dynamics, and virtual testing of vehicle technology, including automated systems.